A&A 527, A69 (2011)
DOI: 10.1051/0004-6361/201015878

Astronomy & Astrophysics

H_3O^+ line emission from starbursts and AGNs

S. Aalto[1], F. Costagliola[1], F. van der Tak[2,3], and R. Meijerink[4]

[1] Department of Earth and Space Sciences, Chalmers University of Technology, Onsala Observatory, 43992 Onsala, Sweden
e-mail: saalto@chalmers.se
[2] SRON, Netherlands Institute for Space Research, Landleven 12, 9747 AD Groningen, The Netherlands
[3] Kapteyn Astronomical Institute, University of Groningen, The Netherlands
[4] Leiden Observatory, Leiden University, PO Box 9513, 2300 RA, Leiden, The Netherlands

Received 6 October 2010 / Accepted 15 December 2010

ABSTRACT

Context. The H_3O^+ molecule probes the chemistry and the ionization rate of dense circumnuclear gas in galaxies.
Aims. We use the H_3O^+ molecule to investigate the impact of starburst and AGN activity on the chemistry of the molecular interstellar medium.
Methods. Using the JCMT, we have observed the $3_2^+-2_2^-$ 364 GHz line of p-H_3O^+ towards the centres of seven active galaxies.
Results. We have detected p-H_3O^+ towards IC 342, NGC 253, NGC 1068, NGC 4418, and NGC 6240. Upper limits were obtained for IRAS 15250 and Arp 299. We find large H_3O^+ abundances ($N(H_3O^+)/N(H_2) \gtrsim 10^{-8}$) in all detected galaxies apart from in IC 342 where it is about one order of magnitude lower. We note, however, that uncertainties in $N(H_3O^+)$ may be significant due to lack of definite information on source size and excitation. We furthermore compare the derived $N(H_3O^+)$ with $N(HCO^+)$ and find that the H_3O^+ to HCO^+ column density ratio is large in NGC 1068 (24), moderate in NGC 4418 and NGC 253 (4–5), slightly less than unity in NGC 6240 (0.7) and lowest in IC 342 (0.2–0.6). We compare our results with models of X-ray and photon dominated regions (XDRs and PDRs).
Conclusions. For IC 342 we find that a starburst PDR chemistry can explain the observed H_3O^+ abundance. For the other galaxies, the large H_3O^+ columns are generally consistent with XDR models. In particular for NGC 1068 the elevated $N(H_3O^+)/N(HCO^+)$ ratio suggests a low column density XDR. For NGC 4418 however, large HC_3N abundances are inconsistent with the XDR interpretation. An alternative possibility is that H_3O^+ forms through H_2O evaporating off dust grains and reacting with HCO^+ in warm, dense gas. This scenario could also potentially fit the results for NGC 253. Further studies of the excitation and distribution of H_3O^+ – as well as *Herschel* observations of water abundances – will help to further constrain the models.

Key words. galaxies: evolution – galaxies: starburst – galaxies: active – radio lines: galaxies – ISM: molecules

1. Introduction

Molecular line emission is an important tool for probing the highly obscured inner regions of starburst galaxies and buried AGNs. Line ratios within and between species help determine physical conditions and chemistry of the gas, which provide essential clues to the type and evolutionary stage of the nuclear activity. Important extragalactic probes of cloud properties include molecules such as HCN, HCO^+, HNC, CN, and HC_3N (e.g. Costagliola & Aalto 2010; Krips et al. 2008; Graciá-Carpio et al. 2008; Loenen et al. 2008; Imanishi et al. 2004; Gao & Solomon 2004; Aalto et al. 2002) that trace the dense ($n \gtrsim 10^4$ cm^{-3}) star forming phase of the molecular gas. HCN, HNC, HCO^+ and CN are all species that can be associated both with photon dominated regions (PDRs) (e.g. Tielens & Hollenbach 1985) in starbursts and X-ray dominated regions (XDRs) (e.g. Maloney et al. 1996; Meijerink & Spaans 2005) surrounding active galactic nuclei (AGN). In contrast, HC_3N requires shielded dense gas to survive in significant abundance since it is destroyed by UV and particle radiation (e.g. reactions with the ions C^+ and He^+) (Prasad & Huntress 1980; Rodriguez-Franco et al. 1998, e.g.). These ions are expected to be abundant in for example XDRs. Thus HC_3N line emission may identify galaxies where the starburst is in the early, embedded, stage of its evolution. There is still, however, substantial dichotomy in the interpretation of the line emission from the above molecules and therefore new tracer species to combine with existing information are important.

The hydronium ion H_3O^+ is a key species in the oxygen chemistry of dense molecular clouds, and useful as a measure of the ionization degree of the gas (Phillips et al. 1992). Since H_3O^+ formation requires H_2O to exist in the gas-phase, the H_3O^+ molecule acts as a natural filter to select hot ($T > 100$ K) molecular gas, and therefore traces more specific regions than molecules usually surveyed towards other galaxies. The chemistry of this filtering is the evaporation of icy grain mantles at $T \approx 100$ K (van der Tak et al. 2006b), or that H_2O forms in the gas phase at high ($T > 300$ K) temperatures.

Observations of H_3O^+ emission will therefore help probe the location of dense, warm and active gas in galactic nuclei. Combined with information on the H_2O abundance, these observations may further be used to trace the ionization rate by cosmic rays (produced in supernovae, i.e., starbursts) and/or X-rays (from an AGN). Studies by van der Tak et al. (2006a) have demonstrated this use of H_3O^+ for Sgr B2 in the Galactic centre. Furthermore, recent *Herschel* observations of Galactic sources show 984 GHz $0_0^- - 1_0^+$ H_3O^+ absorption in the diffuse gas towards G10.6-0.4 (W31C) (Gerin et al. 2010) and 1.03–1.63 THz H_3O^+ emission from the high mass star forming region W3IRS5 (Benz et al. 2010). In general H_3O^+ abundances agree well with expectations from PDR models and – together with H_2O^+ and

Table 1. Sample galaxies[a].

Galaxy	α (J2000) hh mm ss	δ (J2000) ° ′ ″	$L_{\rm FIR}$ $L_\odot$	D Mpc
IC 342	03:46:48.00	+68:05:46.0	6×10^8	1.8
NGC 253	00:47:33.12	–25:17:17.59	2.1×10^{10}	2.6
NGC 1068[d]	02:42:40.71	–00:00:47.8	2×10^{11}	14.4
NGC 4418	12:26:54.63	–00:52:39.6	8×10^{10}	27.3
NGC 6240	16:52:58.89	+02:24:03.4	3.5×10^{11}	107
IRAS 15250	15:26:59.40	+35:58:38.0	1.12×10^{12}	244
Arp 299	11:28:33.13	+58:33:58.0	8×10^{11}	42

Notes. [(a)] References: IC 342: Downes et al. (1992); NGC 253: Strickland et al. (2004); NGC 1068: Telesco et al. (1984); NGC 4418: Ridgway et al. (1994); NGC 6240: Yun & Carilli (2002); IRAS15250: Veilleux et al. (1999); Arp 299: Aalto et al. (1997).

OH^+ – provide important further insight into gas phase oxygen chemistry.

Recently we have detected $3_2^+–2_2^-$ H_3O^+ in the nearby starburst M 82 and the ultraluminous galaxy Arp 220 (van der Tak et al. 2008). Derived column densities, abundances, and H_3O^+/H_2O ratios indicate ionization rates similar to or even exceeding that in the Galactic centre. In M 82 the extended evolved starburst (PDR) is a likely source of this ionization rate while, for the ULIRG Arp 220, an AGN-origin (XDR) is suggested.

In the XDR and PDR models grain-processing is not taken into account since the chemistry is taking place in the gas phase. However, a formation route for H_3O^+ involving the evaporation (or removal by shocks) of H_2O from grain surfaces need also to be considered. For example, evaporating H_2O reacting with HCO^+ may provide an important source of H_3O^+ (e.g. Phillips et al. 1992; van der Tak & van Dishoeck 2000).

We have used the James Clerk Maxwell Telescope (JCMT) in Hawaii to observe the $J_K = 3_2^+–2_2^-$ 364 H_3O^+ line (upper level energy $E_u = 139$ K) in seven starburst and active galaxies which cover a range of environments. Our goal is to use H_3O^+ as a tracer of gas properties in galactic nuclei and to see if H_3O^+ can serve as a diagnostic tool to distinguish AGN from starburst activity. In Sects. 2–4 the sample, observations and their results are presented. H_3O^+ line parameters are presented in Sect. 4.1 and in Sect. 4.2 H_3O^+ column densities and fractional abundances are calculated. In Sects. 5.1 and 5.2 H_3O^+ abundances in the context of X-ray and UV irradiated models are discussed and in 5.3 the potential importance of grain chemistry. In the last Sect. 5.5, we present a brief future outlook.

2. The sample

We have selected a sample consisting of seven nearby luminous starburst and AGNs – and one distant ULIRG. The galaxies are selected from their bright HCN line emission. From our previous experience with extragalactic H_3O^+ we knew that the line is weaker than the standard high density gas tracers such as HCN and HCO^+ so we restricted ourselves to a relatively small sample of seven objects (coordinates, FIR luminosities and distances are presented in Table 1):

IC 342 is a nearby barred Scd galaxy of moderate luminosity (central 400 pc has $L_{\rm FIR}$ of 6×10^8 $L_\odot$) with a central starburst. Within its central 300 pc (30″) two molecular arms end in a clumpy central ring of dense gas (e.g. Downes et al. 1992) which surrounds a young star cluster. The ring is suggested to outline the $X2$ orbits in a larger-scale bar. The chemistry of IC 342 has been investigated in detail in a high-resolution study by Meier & Turner (2005). They find that the chemistry in the ring is a mixture of PDR-dominated regions and regions of younger star-forming clouds. The chemistry in the bar/arms is dominated by shocks as shown by CH_3OH (Meier & Turner 2005) and SiO (Usero et al. 2006). Five (A–E) giant molecular clouds (GMCs) are found in the ring and arms. The 13″ JCMT beam of our H_3O^+ observations is pointed towards the region of GMC B – but also includes GMCs A and E. *GMCs B and C are the sites of young (a few Myr) star formation and are also the regions where incoming molecular clouds meet the ring. GMC A has more PDR-like characteristics.* The dust temperature of IC 342 is estimated to 42 K (e.g. Becklin et al. 1980).

NGC 253 is also a nearby barred galaxy located in the Sculptor group with a compact nuclear starburst and a IR luminosity that appears to originate in regions of intense massive star formation within its central few hundred parsecs (Strickland et al. 2004). From their 2 mm spectral scan Martín et al. (2006) suggest that the chemistry of NGC 253 shows strong similarities to that of the Galactic centre molecular region, which is thought to be dominated by low-velocity shocks. High resolution SiO observations show bright emission resulting from large scale shocks as well as gas entrained in a nuclear outflow (García-Burillo et al. 2000). Note also that it is suggested that NGC 253 is a galaxy in which a strong starburst and a weak AGN coexist (e.g. Weaver et al. 2002; Müller-Sánchez et al. 2010). High resolution observations of HCN and HCO^+ 1–0 (Knudsen et al. 2007) show strongly centrally concentrated emission. The 13″ JCMT beam covers the bulk of the nuclear emission from HCN and HCO^+. The central dust temperature of NGC 253 is estimated to 50 K (Melo et al. 2002).

NGC 1068 is the nearest example of a type 2 Seyfert galaxy luminous in the infrared. Surrounding the AGN there is a 4″ circumnuclear molecular ring or -disk (CND) and on a larger scale there is a NIR stellar bar 2.3 kpc long. This bar is connected to a large-scale, molecular starburst ring that contributes about half the bolometric luminosity of the galaxy (e.g. Telesco et al. 1984; Scoville et al. 1988; Tacconi et al. 1994; Helfer & Blitz 1995; Tacconi et al. 1997). Bright HCN 1–0 line emission is observed towards the CND while the HCO^+ 1–0 emission is relatively fainter by a factor of 1.5 (e.g. Kohno et al. 2001). Only the CND and a fraction of the bar is covered by our JCMT beam and we adopt a source size of 2″ for the CND. The dust of the inner 4″ appears to show a strong temperature gradient – from about 800 K in the very inner region to 150–275 K at a distance of 0.″8 or greater (Tomono et al. 2006). Alloin et al. (2000) find temperatures of about 150 K 200 pc from the nucleus. There is a also radio jet from the nucleus which falls into our JCMT beam (e.g. Wilson & Ulvestad 1983).

NGC 4418 is a luminous, edge-on, Sa-type galaxy with a deeply dust-enshrouded nucleus (Spoon et al. 2001). NGC 4418 is a FIR-excess galaxy with a logarithmic IR-to-radio continuum ratio (q) of 3 (Roussel et al. 2003). This excess may be caused by either a young pre-supernova starburst or a buried AGN (Aalto et al. 2007; Roussel et al. 2003; Imanishi et al. 2004). Unusually luminous HC_3N line emission (Aalto et al. 2002, 2007; Costagliola & Aalto 2010) has been interpreted as a signature of young starburst activity. Mid-IR intensities are indicative of dust temperatures of 85 K (Evans et al. 2003) inside a radius of 50 pc (0.″5). The IR luminosity-to-molecular gas mass ratio is high for a non-ULIRG galaxy indicating that

intense, compact activity is hidden behind the dust. Recent high resolution imaging of CO 2–1 (Costagliola et al., in prep.) indicate a molecular source size of 0.″5.

NGC 6240 is an infrared luminous merger of two massive spiral galaxies. Two AGN/LINER nuclei are separated by 1″ and the bulk of the molecular gas has piled up between the two nuclei (Iono et al. 2007; Tacconi et al. 1999). Luminous HCO^+ 4–3 emission is also emerging from in between the two nuclei where the H_2 emission is also located. The mid-IR sources (24.5 μm) are associated with the two X-ray nuclei – the brightest by far being the southern nucleus (T = 55–60 K) (Egami et al. 2006). It has been suggested that the medium between the two nuclei is dominated by starburst superwinds from the southern nucleus (Ohyama et al. 2000) and the molecular gas is indeed highly turbulent (Iono et al. 2007; Tacconi et al. 1999). The JCMT beam encompasses the entire molecular structure of this galaxy and we adopt a source size of 1″ for the H_3O^+ emission.

IRAS 15250+3609 is a relatively distant ultraluminous galaxy – probably a major merger with a dominant bright nucleus. A tidal feature appears to emerge from the southwest side of the nucleus and turns around on the eastern side to create an enormous closed ring, 27 kpc in diameter. The optical spectrum is a composite of H II and LINER features (Veilleux et al. 1999). IRAS 15250 exhibits deep silicate absorption features (Spoon et al. 2006) indicating a deeply enshrouded nucleus. Our JCMT beam covers the whole optical galaxy.

Arp 299 is an IR-luminous merging system of two galaxies, IC 694 and NGC 3690. Strong ^{12}CO emission has been detected from the nuclei of IC 694 and NGC 3690 and from the interface between the two galaxies (e.g. Sargent & Scoville 1991; Aalto et al. 1997). The two nuclei, as well as the western overlap region, currently undergo intense star formation activity (e.g. Gehrz et al. 1983). Bright HCN 1–0 emission is emerging from both nuclei as well as from the overlap region (e.g. Aalto et al. 1997). Water emission from NGC 3690 suggests that it also harbours an AGN (Tarchi et al. 2007). To cover all three regions a map was carried out.

3. Observations

The 364.7974 GHz $J_K = 3_2^+ - 2_2^-$ line of H_3O^+ was observed towards the sample galaxies in February and August 2008, with the James Clerk Maxwell Telescope (JCMT[1]) on Mauna Kea, Hawaii. We used the 16 elements heterodyne array HARP. Each of the receptors of the array has a beam size of 14″ at 345 GHz and the sources were placed in the receptor labeled H05[2]. The back end was the Auto-Correlation Spectrometer and Imaging System (ACSIS), providing 1.0 GHz bandwidth in 2048 channels and a maximum resolution of 0.4 km s^{-1}. In order to optimize baseline stability, double beam switching at a rate of 1 Hz was used with an offset of 120″. Weather conditions were optimal, with about 1 mm of precipitable water vapor, leading to a typical noise rms of 2 mK at 10 km s^{-1} resolution. Telescope pointing was checked every hour on the CO line emission of nearby AGB stars and always found to be within 2″. Data were extracted into fits files with the starlink software and analyzed in CLASS. Linear baselines were subtracted, line parameters were calculated by fitting Gaussian profiles to the spectra. The resulting spectra are shown in Fig. 1. Throughout this paper, velocities are in the heliocentric frame and redshift is computed using the radio convention.

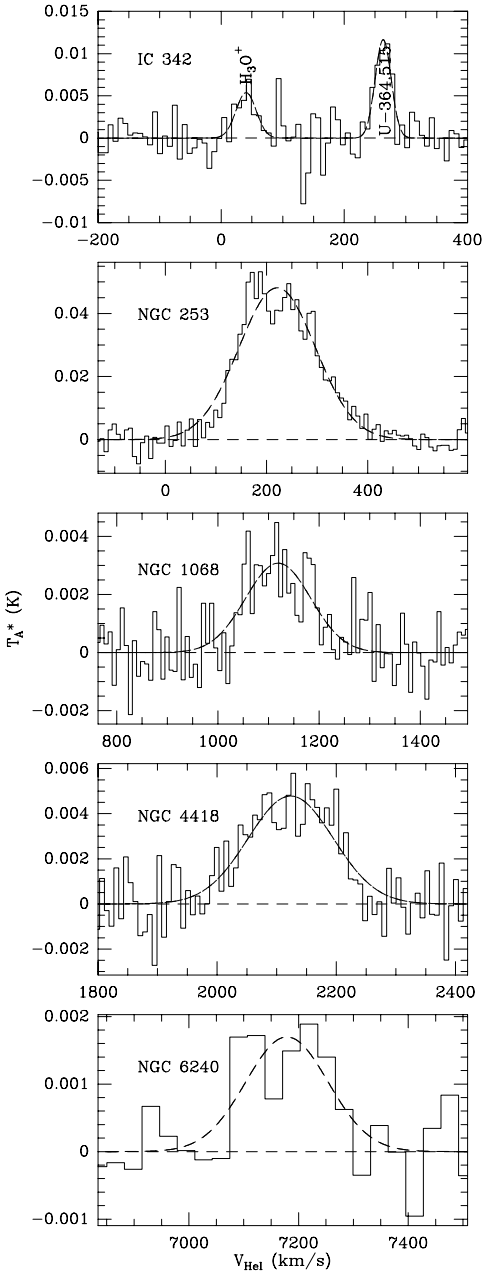

Fig. 1. Observed spectra of H_3O^+. The intensity scale is in T_A^*, not corrected for the JCMT beam efficiency, that at this frequencies is 0.7. The parameters of the detected lines were obtained by Gaussian fits, shown on the plots as dashed lines.

4. Results

4.1. Line intensities and line widths

Integrated line intensities, line widths and fitted velocities (heliocentric) for the seven observed galaxies can be found in

[1] The JCMT is operated by the Joint Astronomy Centre on behalf of the Science and Technology Facilities Council of the United Kingdom, the Netherlands Organization for Scientific Research, and the National Research Council of Canada.

[2] For more information see: www.jach.hawaii.edu/JCMT/spectral_line/Instrument_homes/HARP/HARP.html

Table 2. H_3O^+ line results[a].

Galaxy	$\int T_A^*$ [K km s^{-1}]	V_{line} [km s^{-1}]	δV [km s^{-1}]	T_A^* [mK]
IC 342				
08-2008:[b]				
H_3O^+	0.30 ± 0.07	39 ± 10	75 ± 18	3.7
02-2008:[b]				
H_3O^+	0.22 ± 0.06	40 ± 5	39 ± 13	5.4
(U-line	0.38 ± 0.05	263 ± 2	30 ± 5	11.6)
NGC 253	9.35 ± 0.18	221 ± 2	180 ± 4	48.8
NGC 1068[d]	0.52 ± 0.05	1120 ± 8	160 ± 20	3.0
NGC 4418	1.02 ± 0.06	2129 ± 5	171 ± 11	5.6
NGC 6240	0.32 ± 0.05	7179 ± 15	177 ± 27	1.7
IRAS 15250	<0.012[c]	...	...	<1.0
Arp 299	<0.020[d]	...	...	<2.0

Notes. [(a)] Integrated line intensities and peak line intensities are given in T_A^*, η_{mb} is 0.65–0.7 and we have adopted 0.7 here for conservative values of $N(H_3O^+)$. [(b)] Data reduction of H_3O^+ and U-line taken at JCMT 02-2008 and 08–2008. [(c)] 1σ upper limit for a *FWHM* linewidth of 500 km s^{-1}. [(d)] 1σ upper limit for a *FWHM* linewidth of 300 km s^{-1}. The pointing centre of HARP was in between the two nuclei. We added the spectra in the three emission regions of Arp 299 covered by HARP to produce a spectrum with a 1σ upper limit of 2 mK.

Table 2. p-H_3O^+ line emission was detected towards IC 342, NGC 4418, NGC 253, NGC 1068 and NGC 6240, while Arp 299 and IRAS 15250 were not detected.

In general it is found that line widths and shapes (Fig. 1) agree well with those found for HCN and HCO^+ in the central regions of the systems (Nguyen et al. 1992; Aalto et al. 2007; Knudsen et al. 2007). The most noteworthy deviation from this is NGC 6240 where the linewidth of HCN and HCO^+ (Greve et al. 2009) is more than a factor of two greater than what we find for H_3O^+. A possible explanation for this could be the weak H_3O^+ signal resulting in a moderate signal-to-noise profile. For NGC 1068 the line width agrees well with that of HCO^+ 4–3 but is somewhat narrower than what is observed for HCN 4–3 (202 km s^{-1}) (Pérez-Beaupuits et al. 2009).

For IC 342 an unidentified (U) line was detected in February 2008 – but it did not appear again in August the same year. The line is somewhat narrower than the H_3O^+ line and appear at a velocity of 263 km s^{-1} (rest frequency 364.477 GHz). It is possible that it is an atmospheric O_3 line.

4.2. Column densities, excitation and abundances

Since we have no direct information on the excitation of the H_3O^+ molecule we make some assumptions that will have to be tested in future observations. The critical density of the H_3O^+ transition is high (about $n_{crit} = 10^6$ cm^{-3}, Phillips et al. 1992) and the low reduced mass of the H_3O^+ molecule makes its excitation very sensitive to radiative pumping by dust. We therefore assume that the coupling between the colour temperature of the IR emission and the excitation temperature of H_3O^+ holds as long as the dust colour temperature is above 30 K (see discussion in van der Tak et al. 2008).

For each galaxy we ran a RADEX model (van der Tak et al. 2007) with temperatures ranging from $T = 10$–500 K. In these calculations, the volume density is set to an arbitrary large value, so that the excitation of H_3O^+ is thermalized. The adopted excitation temperature is essentially the radiation temperature and a radiative excitation with one excitation temperature is simulated. We therefore do not use the full non-LTE capacity of RADEX.

The results are shown in Fig. 2. Each plot has temperature (kinetic or radiation) on the x axis and H_3O^+ column on the y axis. The contour line corresponds to the observed brightness temperature. This depends on our assumption for the source size.

H_3O^+ abundances relative to H_2 ($X(H_3O^+)$) are listed in Table 3. We have used CO 2–1 spectra from the literature and used a Galactic conversion factor from CO luminosity to H_2 mass (2.5×10^{20} cm^{-2} K^{-1} km^{-1} s) to estimate $N(H_2)$. Note that for Galactic nuclei (and starbursts) it is argued that this conversion factor overestimates the H_2 column density by factors of 5–10 (see e.g. Martín et al. (2010)). Since we wish to reduce the risk of overestimating the H_3O^+ abundances we have however still adopted the standard conversion factor. For IC 342 and NGC 253 we have estimated and average $N(H_2)$ for the 13″ beam size. For NGC 1068, NGC 4418 and NGC 6240 we have used the same adopted source size as for H_3O^+.

4.2.1. Errors in H_3O^+ column density and abundances

Our assumptions on the excitation and spatial extent of H_3O^+ introduce errors in the column density estimates. For IC 342 in particular the source size error can be significant. We assume that the source fills the beam which gives us an average column density for GMCs A, B and E, but the real column density towards a particular cloud should be higher. For NGC 253 the double peaked line shape suggests that the H_3O^+ emission is emerging from both dense-gas peaks in the centre and is filling the JCMT beam. For NGC 1068 the H_3O^+ source size in the CND could be anything from <1″ to 4″. We have assumed a source size of 2″. For NGC 4418 and NGC 6240 the source sizes are $\lesssim$1″ which means that the beam dilution is significant, but no H_3O^+ emission is missed.

In Fig. 2 the impact of the assumption of the excitation temperature on the resulting H_3O^+ column density is illustrated. Note the strong dependence of $N(H_3O^+)$ for $T_{ex} \lesssim 60$ K. For NGC 253 (for example) N(p-H_3O^+) changes from 9×10^{14} cm^{-2} when $T_{ex} = 50$ K to 7×10^{15} for $T_{ex} = 25$ K. When T_{ex} exceeds 60 K, however, the temperature dependence on $N(H_3O^+)$ is almost gone. Thus for all galaxies, except IC 342, we are not likely to overestimate $N(H_3O^+)$ by more than a factor of 2 since the adopted $T_{ex} \gtrsim 50$ K. It is possible that H_3O^+ could be collisionally excited. In this case the excitation temperature is likely significantly lower than the ones we assume here (beacuse of the high critical density). In Fig. 2 it is evident that the $N(H_3O^+)$ would go up considerably with decreasing temperature. With the assumed T_{ex} the resulting $N(H_3O^+)$ is already quite large for all galaxies – even larger H_3O^+ columns would be an interesting result indeed, but very difficult to explain with current models. The excitation can be constrained through observing multiple transitions and Requena-Torres et al. (in prep.) are currently studying the 307 and 364 GHz line of H_3O^+ in a sample of starburst galaxies.

We conclude that the source size uncertainties dominate the errors in the column density calculations. To improve future $N(H_3O^+)$ calculations it is necessary to determine source sizes through high resolution observations and to obtain information on $T_{ex}(H_3O^+)$ through multi-transition observations.

In addition it should be noted that the estimates of the H_3O^+ relative abundances are dependent on the reliability of the conversion factor from CO luminosity to H_2 mass.

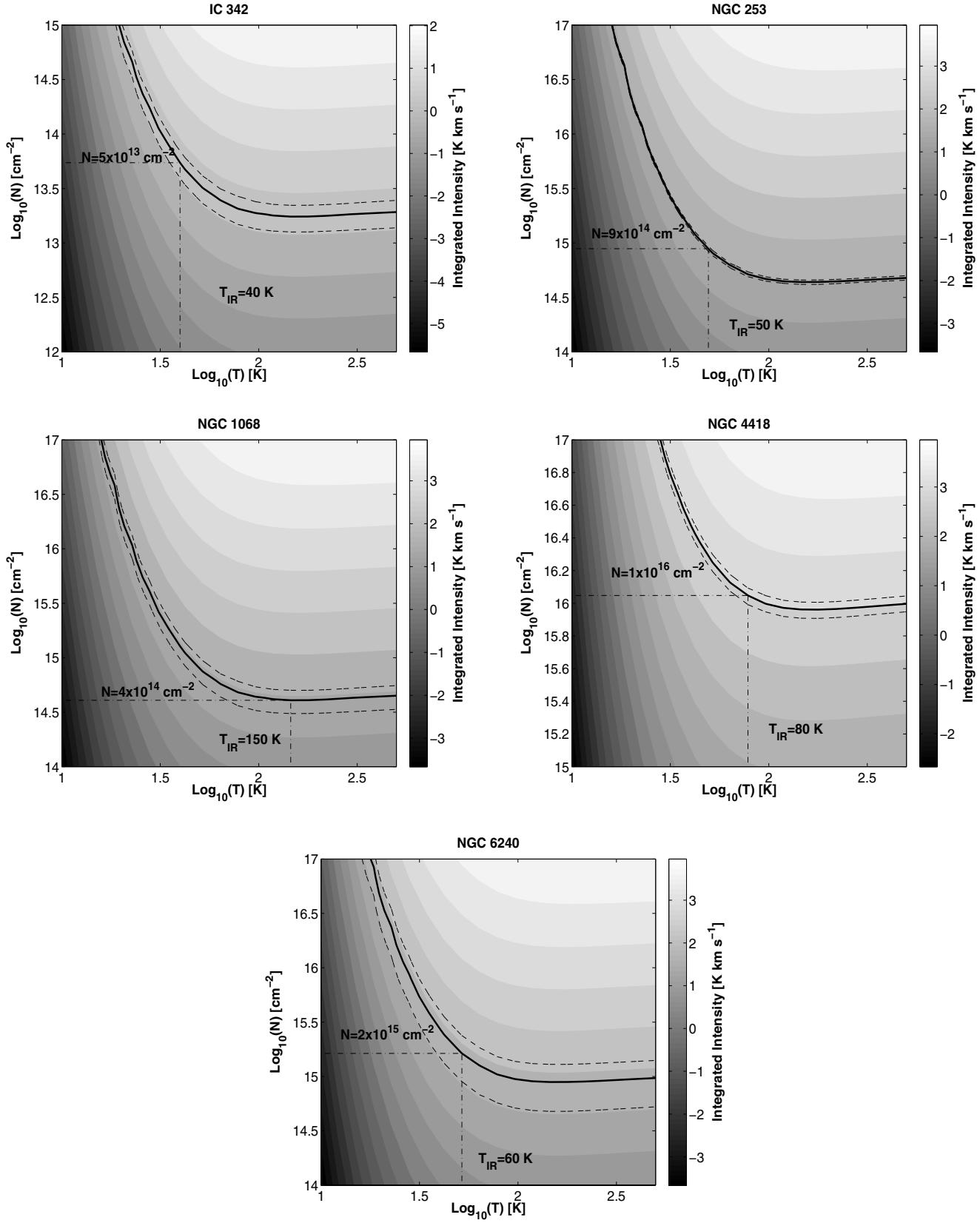

Fig. 2. On the *x* axis we find the temperature of the exciting background radiation and on the y axis the column density of H_3O^+. For each galaxy, the brightness temperature of the H_3O^+ transition is shown in a gray scale map. The thick black contour marks the observed value, with one sigma errors marked by dashed lines. Background temperatures estimated by IR observations are also reported and used to derive a column density consistent with the observed brightness temperature. Note that the column density fits include only the para column.

Table 3. Parameters[a] for the RADEX modeling of the H_3O^+ Line.

Galaxy	Source size[b] [″]	T_{IR} [K]	$N(H_3O^+)$[c] fit [cm^{-2}]	$X(H_3O^+)$[d]
IC 342	13	40	1.25×10^{14}	4×10^{-9}
NGC 253	13	50	2.25×10^{15}	1.5×10^{-8}
NGC 1068	2	150	1×10^{15}	1×10^{-8}
NGC 4418	0.5	80	2.5×10^{16}	3×10^{-8}
NGC 6240	1	50	5×10^{15}	2.5×10^{-8}

Notes. [(a)] The temperature range investigated for all galaxies was 10–500 K, but solutions were fixed where $T_{ex} = T_{IR}$. The $N(H_3O^+)$ range searched was 10^{12}–10^{17} cm^{-2}. [(b)] For a discussion of adopted source sizes see Sect. 2. [(c)] The total beam-averaged column density of H_3O^+ is 2–3 times higher than that of p-H_3O^+ in Fig. 2, because the ortho to para ratio of H_3O^+ drops from the high-temperature limit of *o/p* = 1 for $T > 100$ K to *o/p* = 2 when $T < 50$ K. Here we have corrected column densities for an *o/p* ratio of 1.5. [(d)] *IC 342:* $N(H_2)$ is estimated to 3×10^{22} cm^{-2} (from the CO data of Eckart et al. 1990). *NGC 253:* $N(H_2)$ is estimated to 1.3×10^{23} cm^{-2} (using CO data from Mauersberger et al. (1996). *NGC 1068:* From Tacconi et al. (1994) the $N(H_2)$ for the CND is estimated to be $2-10 \times 10^{22}$ cm^{-2}. If we take the CO 2–1 data from Planesas et al. (1989) and assume a source size of 2″ we obtain $N(H_2) = 1.35 \times 10^{23}$ cm^{-2}. *NGC 4418:* Column density for H_2 for a 0.″5 CO 2–1 source size is $N(H_2) = 7.4 \times 10^{23}$ cm^{-2} (Costagliola et al. in prep.). *NGC 6240:* Iono et al. (2007) estimate $N(H_2)$ to 1×10^{23} cm^{-2} from their CO 3–2 data.

5. Discussion

5.1. H_3O^+ abundances and PDR/XDR models

We compare the column densities of H_3O^+ and H_2 in Table 3 to chemical models of clouds irradiated by either far-UV, photon dominated regions (PDRs) or X-ray photons (XDRs). In general, we expect the XDRs to dominate in molecular ISMs surrounding an AGN. The XDR and PDR models we use are presented in Meijerink & Spaans (2005) and Meijerink et al. (2007). In general, the thermal and chemical structure of XDRs and PDRs are different. Larger parts of an XDR can be maintained at high temperaure and the ionization fraction of an XDR can be up to two orders of magnitude higher ($x_e = 10^{-2}$–10^{-1}) than in a PDR. In an XDR H_2O may form in the gas phase at high temperatures (200–300 K) and then react with either H_3^+ or HCO^+ to form H_3O^+.

Source averaged HCO^+ abundances are typically $\approx 10^{-8}$ for all detected galaxies except for IC 342. A general result of the models presented in van der Tak et al. (2008) is that the $X(H_3O^+)$ does not exceed 3×10^{-9} in PDRs – even in the models with an extremely high cosmic-ray ionization rate of $\zeta = 5.0 \times 10^{-15}$ s^{-1}. H_3O^+ abundances approaching 10^{-8} and beyond are more likely to occur in X-ray dominated regions and we conclude that *the XDR scenario fits the $X(H_3O^+)$ values of NGC 253, NGC 1068, NGC 4418 and NGC 6240. For IC 342, the results are consistent with a PDR, but a model with a high ζ of* 5.0×10^{-15} s^{-1}.

5.1.1. Water abundances

The H_3O^+/H_2O ratio is an even better probe of the ionization rate, and potential nature of the emitting source. It is straight forward to obtain H_3O^+/H_2O abundance ratios as large as 10^{-2} in XDR models, while for PDR models ratios are generally 10^{-3} or less. *Herschel* has already measured water abundances in M 82 (Weiß et al. 2010) (see also Sect. 5.4) and results for other galaxies will follow soon.

5.2. Relative H_3O^+ and HCO^+ abundances and XDR/PDR models

Kohno et al. (2001) and Imanishi et al. (2004) find HCN/HCO^+ 1–0 line intensity ratios greater than unity in several Seyfert nuclei – where also the HCN/CO 1–0 line ratio is high. Furthermore, Graciá-Carpio et al. (2006) find elevated HCN/HCO^+ 1–0 line ratios in ULIRGs. This is often interpreted as a sign of an underabundance of HCO^+ compared to HCN due to X-ray chemistry. (Although it is important to remember that an abundance difference cannot be unambiguously deduced from a single-transition line ratio). Underabundant HCO^+ in XDRs has been proposed in theoretical work by Maloney et al. (1996). However, more recent models by Meijerink & Spaans (2005) suggest that HCO^+ may be underabundant in moderate column density ($N_H < 10^{22.5}$ cm^{-2}) XDRs – but for larger columns the reverse is true and $X(HCO^+)$ generally exceeds $X(HCN)$. Here we compare our derived $N(H_3O^+)$ with $N(HCO^+)$ for the sample galaxies to see if large H_3O^+ abundances are paired with a particularly low HCO^+ abundance, and to compare $N(H_3O^+)/N(HCO^+)$ with the expectations from current models.

In the XDR/PDR models, the formation of both H_3O^+ as well as HCO^+ is mainly driven by reactions with H_2, H_2^+, and H_3^+, and destruction by electrons, unless the electron fractional abundance is very low $x_e \lesssim 10^{-7}$–10^{-8}. However, the interpretation of an $N(H_3O^+)/N(HCO^+)$ abundance ratio in an XDR/PDR scenario is not entirely straightforward, but the models provide some useful limits. For example, in the PDR models H_3O^+/HCO^+ ratios are unlikely to become larger than 3 (Meijerink et al. 2010), while for the XDR models it is quite straightforward to obtain $N(H_3O^+) > N(HCO^+)$, but the obtained ratio is very column density dependent. When the column densities are small (e.g $N(H) \approx 10^{22}$ cm^{-2}) ratios as large as 20 can be obtained, but abundances (and associated brightness temperatures) are small, and in order to obtain significant HCO^+ and H_3O^+ column densities larger clouds are needed. However, when increasing the column, the H_3O^+/HCO^+ column density ratio slowly decreases, but moderate ratios around 4–5 are easy to reproduce with the XDR model.

5.2.1. $N(H_3)/N(HCO^+)$ in the sample galaxies

In Table 4 we list $N(HCO^+)$ and $N(H_3O^+)/N(HCO^+)$ for the sample galaxies. The largest $N(H_3O^+)/N(HCO^+)$ value is found in NGC 1068 which has a Seyfert nucleus and its inner few hundred pc has been suggested to be an XDR (e.g. Usero et al. 2004; Pérez-Beaupuits et al. 2009; García-Burillo et al. 2010). The large abundance ratio of ≈24 suggested for NGC 1068 is consistent with (a low column density) XDR.

For NGC 4418 and NGC 253 XDR models can explain the H_3O^+/HCO^+ ratios (but we note that the values with errors are also within the range of PDR models). For NGC 253 there is evidence that both an AGN and a young starburst is present while for NGC 4418 the nuclear activity is so obscured that the nature of the activity cannot be discerned (see Sect. 2). The H_3O^+/HCO^+ ratio for IC 342 is consistent with a PDR model as is the relative H_3O^+ abundance.

For NGC 6240 the H_3O^+/HCO^+ ratio is consistent with both XDR and PDR models while the H_3O^+ relative abundance favours an XDR. It is interesting to note that even if the molecular gas of NGC 6240 is collected in-between the two nuclei, their radiation could still impact the gas. The two AGNs are separated by 1.″5 which means that the molecular gas is irradiated

Table 4. HCO^+/H_3O^+ ratios.

Galaxy	$N(HCO^+)^a$ [cm^{-2}]	$N(H_3O^+)/N(HCO^+)$
IC 342	$2–6 \times 10^{14}$	0.2–0.6
NGC 253	5×10^{14}	4
NGC 1068	4×10^{13}	24
NGC 4418	4.7×10^{15}	5
NGC 6240	$3 - 4 \times 10^{15}$	0.7

Notes. [(a)] *IC 342*: estimated from Nguyen et al. (1992)(Note that a low $HCO^+/H^{13}CO^+$ 1–0 line ratio of 7 suggests that HCO^+ columns may be higher. *NGC 253*: from Martín et al. (2006) (6.5×10^{13} for T_{ex} = 12 K and for 35″ source size. Rescaled $N(HCO^+)$ for the 10″ by 14″ H_3O^+ source size of Knudsen et al. 2007). *NGC 1068*: we used the data provided in Pérez-Beaupuits et al. (2009) and made a rotational diagram (assuming a 2″ source size) finding $T_{ex}(HCO^+)$ = 36 K. *NGC 4418*: column density for HCO^+ (based on data in Aalto et al. (2007) and unpublished JCMT HCO^+ 4–3 data) for a 0.″5 source size. *NGC 6240:* We estimate the HCO^+ column density from the excitation information given in Iono et al. (2007) and for a source size of 1″.

by intense X-ray emission from two directions on only 370 pc distance. This scenario could possibly explain both the relatively high H_3O^+ and HCO^+ abundances.

5.3. Grain chemistry and the formation of H_3O^+

Above we have found that the XDR/PDR models can potentially explain the H_3O^+ and HCO^+ column densities and abundances we found for the observed galaxies. However, for NGC 4418 the problem with an XDR explanation is the large column densities of gas and dust observed towards its centre (see footnote of Table 3) where Costagliola & Aalto (2010) find global HC_3N abundances similar to those found towards hot cores in Sgr B2. Intense vibrational line emission suggest that the HC_3N indeed exists in warm-to-hot environments in the very centre of the galaxy. The HC_3N abundances are not consistent with either XDRs or PDRs.

Thus, we have searched for alternative explanations to the H_3O^+ line emission outside of the XDR and PDR models. Elevated HC_3N line emission is consistent with the conditions in warm, dense shielded gas associated with embedded star formation. Is it then possible to obtain relative H_3O^+ abundances of $\approx 10^{-8}$ without the X-ray chemistry?

In a scenario where grains are important, the H_2O can evaporate off the grains at temperatures >100 K and in Phillips et al. (1992) the destruction of HCO^+ through the reaction of H_2O is found to be an important formation process for H_3O^+ when the gas is dense and warm. For a water abundance $X(H_2O)$ of 10^{-5} and a density $n(H_2)$ of 10^5 cm^{-3} Phillips et al. (1992) find an H_3O^+ abundance, $X(H_3O^+)$, of $\approx 10^{-8}$ and $X(HCO^+)$ a factor 2–3 lower. It is unclear however, if the $N(H_3O^+)/N(H_2O)$ can be greater than 10^{-3} within the context of their model. van der Tak & van Dishoeck (2000) find the same effect in their study of the of Galactic protostar GL 2136. In their Fig. 1 the temperature and density structure is presented including calculated concentrations of HCO^+ both with and without destruction by H_2O.

We suggest that for NGC 4418 it is possible that the H_3O^+ abundance and the $N(H_3O^+)/N(HCO^+)$ ratio can be explained by a model where the gas is warm and dense and water is coming off the grains to react with HCO^+ to form H_3O^+. This process could contribute to a reduction of the HCO^+ abundance in the gas phase which may result in a lower HCO^+ line intensity in any transition. Note that shocks may be responsible for removing the water from the grains making it available for further reactions including H_3O^+ formation. Flower & Pineau Des Forêts (2010) presents models where water abundances are related to the type and strength of shocks and there are a multitide of Galactic observational studies showing enhancement of water emission in shocks (Nisini et al. 2010; Lefloch et al. 2010; Wampfler et al. 2010; Melnick et al. 2008). Apart from causing H_2O to come off the grains, shocks can result in efficient gas-phase formation of H_2O from OH in the shocked high-temperature regime.

5.4. H_2O^+, H_3O^+, and H_2O

Weiß et al. (2010) find a (potentially) surprisingly low $N(H_2O)/N(H_2O^+)$ ratio of only a few which they attribute to H_2O evaporating off the grains through shocks, the H_2O then becomes photodissociated into O and OH. Ion-molecule reactions then make H_2O^+ while H_2O abundances remain low. It is furthermore noteworthy that $X(H_2O^+) > X(H_3O^+)$ in M 82 (van der Tak et al. 2008; Weiß et al. 2010). This is consistent with the low density ($n = 10^3$ cm^{-3}), high cosmic ray rate ($>5 \times 10^{-15}$ s^{-1}) model (Model 2) of Meijerink et al. (2010). This model does however not include any grain processing.

In van der Tak (2010a) a photoevaporation-ionization hypothesis for the $H_3O^+/H_2O^+/H_2O$ ratio is discussed for M 82 noting that testing this theory requires calculation of the photodissociation cross-section of H_3O^+. Whether this hypothesis holds for other galaxies, however, remains to be seen: the H_2O/H_2O^+ ratio in M 82 may well be unusually low. In the ULIRG Mrk 231 $N(H_2O) \gg N(H_2O^+)$ and the H_2O^+ line emission feature is consistent with an XDR interpretation (van der Werf et al. 2010b).

5.5. Future studies

With this study we have confirmed that the 364 GHz line of p-H_3O^+ is feasible to detect in starburst and active galaxies and that H_3O^+ fractional abundances are substantial. The HIFI heterodyne spectrometer onboard ESA's *Herschel* space observatory is currently obtaining H_2O and H_3O^+ data around 1 THz and more accurate estimates of the H_2O/H_3O^+ abundance ratios can be determined for many sources improving the understanding of the ionization rates of nuclear molecular regions. Determining the cource size and excitation of H_3O^+ is essential to further improve the understanding of the impact of the nuclear activity on its surrounding interstellar medium and to facilitate a more accurate comparison with models. In the near future, grain chemistry and impact of shocks should be added to the interpretation of the data. In particular the results for NGC 4418 – and to some degree also NGC 253 – emphasizes this conclusion.

Acknowledgements. We are very grateful to the staff of the JCMT for their help and support and we thank the referee, Santiago Garcia-Burillo, for a thorough and very useful report which improved the paper. This research has made use of the NASA/IPAC Extragalactic Database (NED) which is operated by the Jet Propulsion Laboratory, California Institute of Technology, under contract with the National Aeronautics and Space Administration.

References

Aalto, S., Radford, S. J. E., Scoville, N. Z., & Sargent, A. I. 1997, ApJ, 475, L107
Aalto, S., Polatidis, A. G., Hüttemeister, S., & Curran, S. J. 2002, A&A, 381, 783
Aalto, S., Monje, R., & Martín, S. 2007, A&A, 475, 479

Alloin, D., Pantin, E., Lagage, P. O., & Granato, G. L. 2000, A&A, 363, 926
Becklin, E. E., Gatley, I., Matthews, K., et al. 1980, ApJ, 236, 441
Benz, A. O., Bruderer, S., van Dishoeck, E. F., et al. 2010, A&A, 521, L35
Costagliola, F., & Aalto, S. 2010, A&A, 515, A71
Downes, D., Radford, S. J. E., Guilloteau, S., et al. 1992, A&A, 262, 424
Eckart, A., Downes, D., Genzel, R., et al. 1990, ApJ, 348, 434
Egami, E., Neugebauer, G., Soifer, B. T., et al. 2006, AJ, 131, 1253
Evans, A. S., Becklin, E. E., Scoville, N. Z., et al. 2003, AJ, 125, 2341
Flower, D. R., & Pineau Des Forêts, G. 2010, MNRAS, 406, 1745
Gao, Y., & Solomon, P. M. 2004, ApJS, 152, 63
García-Burillo, S., Martín-Pintado, J., Fuente, A., & Neri, R. 2000, A&A, 355, 499
García-Burillo, S., Usero, A., Fuente, A., et al. 2010, A&A, 519, A2
Gehrz, R. D., Sramek, R. A., & Weedman, D. W. 1983, ApJ, 267, 551
Gerin, M., de Luca, M., Black, J., et al. 2010, A&A, 518, L110
Graciá-Carpio, J., García-Burillo, S., Planesas, P., & Colina, L. 2006, ApJ, 640, L135
Graciá-Carpio, J., García-Burillo, S., Planesas, P., Fuente, A., & Usero, A. 2008, A&A, 479, 703
Greve, T. R., Papadopoulos, P. P., Gao, Y., & Radford, S. J. E. 2009, ApJ, 692, 1432
Helfer, T. T., & Blitz, L. 1995, ApJ, 450, 90
Imanishi, M., Nakanishi, K., Kuno, N., & Kohno, K. 2004, AJ, 128, 2037
Iono, D., Wilson, C. D., Takakuwa, S., et al. 2007, ApJ, 659, 283
Knudsen, K. K., Walter, F., Weiss, A., et al. 2007, ApJ, 666, 156
Kohno, K., Matsushita, S., Vila-Vilaró, B., et al. 2001, in The Central Kiloparsec of Starbursts and AGN: The La Palma Connection, ed. J. H. Knapen, J. E. Beckman, I. Shlosman, & T. J. Mahoney, ASP Conf. Ser., 249, 672
Krips, M., Neri, R., García-Burillo, S., et al. 2008, ApJ, 677, 262
Lefloch, B., Cabrit, S., Codella, C., et al. 2010, A&A, 518, L113
Loenen, A. F., Spaans, M., Baan, W. A., & Meijerink, R. 2008, A&A, 488, L5
Maloney, P. R., Hollenbach, D. J., & Tielens, A. G. G. M. 1996, ApJ, 466, 561
Martín, S., Mauersberger, R., Martín-Pintado, J., Henkel, C., & García-Burillo, S. 2006, ApJS, 164, 450
Martín, S., George, M. R., Wilner, D. J., & Espada, D. 2010, AJ, 139, 2241
Mauersberger, R., Henkel, C., Wielebinski, R., Wiklind, T., & Reuter, H. 1996, A&A, 305, 421
Meier, D. S., & Turner, J. L. 2005, ApJ, 618, 259
Meijerink, R., & Spaans, M. 2005, A&A, 436, 397
Meijerink, R., Spaans, M., & Israel, F. P. 2007, A&A, 461, 793
Meijerink, R., Spaans, M., Loenen, A. F., & van der Werf, P. P. 2011, A&A, 525, A119
Melnick, G. J., Tolls, V., Neufeld, D. A., et al. 2008, ApJ, 683, 876
Melo, V. P., Pérez García, A. M., Acosta-Pulido, J. A., Muñoz-Tuñón, C., & Rodríguez Espinosa, J. M. 2002, ApJ, 574, 709
Müller-Sánchez, F., González-Martín, O., Fernández-Ontiveros, J. A., Acosta-Pulido, J. A., & Prieto, M. A. 2010, ApJ, 716, 1166
Nguyen, Q., Jackson, J. M., Henkel, C., Truong, B., & Mauersberger, R. 1992, ApJ, 399, 521
Nisini, B., Benedettini, M., Codella, C., et al. 2010, A&A, 518, L120
Ohyama, Y., Yoshida, M., Takata, T., et al. 2000, PASJ, 52, 563
Pérez-Beaupuits, J. P., Spaans, M., van der Tak, F. F. S., et al. 2009, A&A, 503, 459
Phillips, T. G., van Dishoeck, E. F., & Keene, J. 1992, ApJ, 399, 533
Planesas, P., Gomez-Gonzalez, J., & Martin-Pintado, J. 1989, A&A, 216, 1
Prasad, S. S., & Huntress, Jr., W. T. 1980, ApJ, 239, 151
Ridgway, S. E., Wynn-Williams, C. G., & Becklin, E. E. 1994, ApJ, 428, 609
Rodriguez-Franco, A., Martin-Pintado, J., & Fuente, A. 1998, A&A, 329, 1097
Roussel, H., Helou, G., Beck, R., et al. 2003, ApJ, 593, 733
Sargent, A., & Scoville, N. 1991, ApJ, 366, L1
Scoville, N. Z., Matthews, K., Carico, D. P., & Sanders, D. B. 1988, ApJ, 327, L61
Spoon, H. W. W., Keane, J. V., Tielens, A. G. G. M., Lutz, D., & Moorwood, A. F. M. 2001, A&A, 365, L353
Spoon, H. W. W., Tielens, A. G. G. M., Armus, L., et al. 2006, ApJ, 638, 759
Strickland, D. K., Heckman, T. M., Colbert, E. J. M., Hoopes, C. G., & Weaver, K. A. 2004, ApJ, 606, 829
Tacconi, L. J., Genzel, R., Blietz, M., et al. 1994, ApJ, 426, L77
Tacconi, L. J., Gallimore, J. F., Genzel, R., Schinnerer, E., & Downes, D. 1997, Ap&SS, 248, 59
Tacconi, L. J., Genzel, R., Tecza, M., et al. 1999, ApJ, 524, 732
Tarchi, A., Castangia, P., Henkel, C., & Menten, K. M. 2007, New Astron. Rev., 51, 67
Telesco, C. M., Becklin, E. E., Wynn-Williams, C. G., & Harper, D. A. 1984, ApJ, 282, 427
Tielens, A. G. G. M., & Hollenbach, D. 1985, ApJ, 291, 722
Tomono, D., Terada, H., & Kobayashi, N. 2006, ApJ, 646, 774
Usero, A., García-Burillo, S., Fuente, A., Martín-Pintado, J., & Rodríguez-Fernández, N. J. 2004, A&A, 419, 897
Usero, A., García-Burillo, S., Martín-Pintado, J., Fuente, A., & Neri, R. 2006, A&A, 448, 457
van der Tak, F. F. S., & van Dishoeck, E. F. 2000, A&A, 358, L79
van der Tak, F. F. S., Belloche, A., Schilke, P., et al. 2006a, A&A, 454, L99
van der Tak, F. F. S., Walmsley, C. M., Herpin, F., & Ceccarelli, C. 2006b, A&A, 447, 1011
van der Tak, F. F. S., Black, J. H., Schöier, F. L., Jansen, D. J., & van Dishoeck, E. F. 2007, A&A, 468, 627
van der Tak, F. F. S., Aalto, S., & Meijerink, R. 2008, A&A, 477, L5
van der Tak, F. 2010a, in Spectroscopy of Molecular Ions in the Laboratory and in Space (SMILES 2010), AIP Conf. Proc., in press [arXiv:1011.0568]
van der Werf, P. P., Isaak, K. G., Meijerink, R., et al. 2010b, A&A, 518, L42
Veilleux, S., Sanders, D. B., & Kim, D. 1999, ApJ, 522, 139
Wampfler, S. F., Herczeg, G. J., Bruderer, S., et al. 2010, A&A, 521, L36
Weaver, K. A., Heckman, T. M., Strickland, D. K., & Dahlem, M. 2002, ApJ, 576, L19
Weiß, A., Requena-Torres, M. A., Güsten, R., et al. 2010, A&A, 521, L1
Wilson, A. S., & Ulvestad, J. S. 1983, ApJ, 275, 8
Yun, M. S., & Carilli, C. L. 2002, ApJ, 568, 88